The cluster structure of the inner crust of neutron stars in the Hartree-Fock-Bogoliubov approach

F. Grill^{a,b}, J. Margueron^c, N. Sandulescu^{d*}

^{a} *Dipartimento di Fisica, Universitá degli Studi di Milano,*

Via Celoria 16, 20133 Milan, Italy

^{b} *Centro de Física Computacional, Department of Physics,*

University of Coimbra, PT-3004-516 Coimbra, Portugal

^{c} *Institut de Physique Nucleaire, Université Paris-Sud, Orsay Cedex, France*

^{d} *National Institute of Physics and Nuclear Engineering, 76900, Bucharest, Romania*

Abstract

We analyse how the structure of the inner curst is influenced by the pairing correlations. The inner-crust matter, formed by nuclear clusters immersed in a superfluid neutron gas and ultra-relativistic electrons, is treated in the Wigner-Seitz approximation. The properties of the Wigner-Seitz cells, i.e., their neutron to proton ratio and their radius at a given baryonic density, are obtained from the energy minimization at beta equilibrium. To obtain the binding energy of baryonic matter we perform Skyrme-HFB calculations with zero-range density-dependent pairing forces of various intensities. We find that the Wigner-Seitz cells have much smaller numbers of protons compared to previous calculations. For the dense cells the binding energy of the configurations with small proton numbers do not converge to a well-defined minimum value which precludes the determination of their structure. We show that for these cells there is a significant underestimation of the binding energy due to the boundary conditions at the border of the cells imposed through the Wigner-Seitz approximation.

* corresponding author (email:sandulescu@theory.nipne.ro)

I. INTRODUCTION

The inner-crust of neutron stars extends from the so-called neutron drip density, $\rho_d \approx 4 \times 10^{11}$ g cm^{-3}, defined as the density where the neutrons start to drip out from the nuclei of the crust, up to a density of about $\rho \approx 1.4 \times 10^{14}$ g cm^{-3} at which there is a transition towards the uniform core matter. The size and the precise density limits of the inner crust depend on the star mass and on the equation of state employed in the star models [1, 2].

The inner-crust matter of non-accreting cold neutron stars is most probably formed by a crystal lattice of nuclear clusters immersed in a sea of low-density superfluid neutrons and ultra-relativisitic electrons. It is generally considered that in most of its part the inner-crust is formed of nuclei-like clusters. More complex "pasta" structures (e.g., rods, plates, bubbles) are expected to be formed in the transition region between the inner crust and the core matter, see for instance Refs. [1, 2] and references therein.

The first microscopic calculation of the inner-crust structure, still used as a benchmark in neutron stars studies (e.g., Refs. [3–5]) was performed by Negele and Vautherin in 1973 [6]. In this work the crystal lattice is divided in spherical cells which are treated in the Wigner-Seitz (WS) approximation. The nuclear matter from each cell is described in the framework of Hartree-Fock (HF) approximation based on the Density Matrix Expansion (DME) [7]. This approach was preferred to the Density-Dependent Hartree-Fock theory [8] in order to reduce computational complication induced by the non-local exchange potential. The parameters of the DME theory were adjusted to reproduce the experimental binding energies of atomic nuclei and the theoretical calculation of infinite neutron matter available at that time. The spin-orbit interaction was taken into account for the protons but neglected for the neutrons. The HF equations were solved in coordinate representation imposing mixed Dirichlet-Neuman boundary conditions at the border of the cells. The properties of the WS cells found in Ref. [6], determined for a limited set of densities, are shown in Table I. The most remarkable result of this calculation is that the majority of the cells have semi-magic and magic proton numbers, i.e., Z=40,50. This indicates that in these calculations there are strong proton shell effects, as in isolated atomic nuclei. However, as seen from Fig. 1 of Ref. [6] the energies corresponding to the cells configurations based on various Z numbers are in fact very close to each other. This fact raises several questions: i) what is the sensitivity of the results on the nuclear interaction, ii) how much the pairing correlations influence the

cells structure, iii) how reliable is the WS approximation.

The effect of pairing correlations on the structure of WS cells was investigated in Ref. [9] within the HF+BCS approach. In the most recent version of these calculations the authors solved the HF+BCS equations with a mixture between the phenomenological functional of Fayans et al [11], employed in the nuclear cluster region, and a microscopical functional derived from Bruckner-Hartree-Fock calculations in infinite neutron matter. The latter was used to describe the neutron gas in the WS cells. In this framework it was found that the cells have not a magic or semi-magic number of protons, as in Ref. [6]. It was also found that pairing can change significantly the structure of the cells compared to HF calculations. These findings show that in order to determine the most probable structure of the inner crust one needs more investigations based on various effective interactions and many-body approximations.

In this study we analyse the effect of pairing on inner crust structure in the Hartree-Fock-Bogoliubov approach (HFB). This approach offers better grounds than HF+BCS approximation for treating pairing correlations in non-uniform nuclear matter with both bound and unbound neutrons. To investigate the dependence of the inner crust structure on pairing, the HFB calculations are performed with three different density-dependent pairing forces adjusted to reproduce various pairing scenarios in nuclear matter.

In principle, the symmetries of the inner crust lattice should be taken properly into account when inner crust structure is determined. Since imposing the exact lattice symmetries in microscopic self-consistent models is a very difficult task (for approximative solutions to this problem see [13] and the references therein) we solve the HFB equations in the WS approximation, as commonly done in inner crust studies [6, 9]. This approximation induces, through the boundary conditions at the border of the cells, an artificial shell structure in the energy spectra of nonlocalized neutrons [10]. The errors caused by the spurious shells, which affect mainly the high density cells, are estimated by using the method proposed in Ref.[16].

The paper is organized as follows: in Section II we describe how the cells energy is calculated in the HFB and WS approximations, in Section III we present the equations for beta equilibrium and in Section IV we discuss the results of the calculations.

II. THE ENERGY OF WIGNER-SEITZ CELLS

As in Ref. [6], the lattice structure of the inner crust is described as a set of independent cells of spherical symmetry treated in the WS approximation. For baryonic densities below $\rho \approx 1.410^{14} g/cm^3$, each cell has in its center a nuclear cluster (bound protons and neutrons) surrounded by low-density and delocalized neutrons and immersed in a uniform gas of ultra-relativistic electrons which assure the charge neutrality. At a given baryonic density the structure of the cell, i.e., the N/Z ratio and the cell radius is determined from the minimization over N and Z of the total energy under the condition of beta equilibrium. The energy of the cell, relevant for determining the cell structure, has contributions from the nuclear and the Coulomb interactions. Its expression is written in the following form

$$E = E_M + E_N + T_e + E_L. \tag{1}$$

The first term is the mass difference $E_M = Z(m_p + m_e) + (N - A)m_n$ where N and Z are the number of neutrons and protons in the cell and A=N+Z. E_N is the binding energy of the nucleons, which includes the contribution of proton-proton Coulomb interaction inside the nuclear cluster. T_e is the kinetic energy of the electrons while E_L is the lattice energy which takes into account the electron-electron and electron-proton interactions. The contribution to the total energy coming from the interaction between the WS cells [12] it is not considered since it is very small compared to the other terms of Eq.(1). Notice also that the gravitational energy is not taken into account in the energy minimization because its variation at the nuclear scale is negligible.

A. The nuclear binding energy in the HFB approach

In the present study the nuclear binding energy of the WS cells is calculated in the framework of HFB approach. For the particle-hole channel we use a Skyrme-type interaction of the standard form [14], i.e.,

$$
\begin{aligned}
V_{\mathrm{Skyrme}}(\mathrm{r_i}, \mathrm{r_j}) =\ & t_0(1 + x_0 P_\sigma)\delta(\mathrm{r}_{ij}) \\
& + \frac{1}{2}t_1(1 + x_1 P_\sigma)\frac{1}{\hbar^2}\left[p_{ij}^2\,\delta(\mathrm{r}_{ij}) + \delta(\mathrm{r}_{ij})\,p_{ij}^2 \right] \\
& + t_2(1 + x_2 P_\sigma)\frac{1}{\hbar^2}\mathrm{p}_{ij}.\delta(\mathrm{r}_{ij})\,\mathrm{p}_{ij}
\end{aligned}
$$

$$+ \frac{1}{6}t_3(1 + x_3P_\sigma)\rho(\mathrm{r})^\gamma \, \delta(\mathrm{r}_{ij})$$

$$+ \frac{\mathrm{i}}{\hbar^2}W_0(\boldsymbol{\sigma_i} + \boldsymbol{\sigma_j}) \cdot \mathrm{p}_{ij} \times \delta(\mathrm{r}_{ij}) \, \mathrm{p}_{ij} \quad , \tag{2}$$

where $\mathrm{r}_{ij} = \mathrm{r}_i - \mathrm{r}_j$, $\mathrm{r} = (\mathrm{r}_i + \mathrm{r}_j)/2$, $\mathrm{p}_{ij} = -\mathrm{i}\hbar(\nabla_i - \nabla_j)/2$ is the relative momentum, and P_σ is the two-body spin-exchange operator. The parameters of the force we have used in this study correspond to the Skyrme force SLy4 [14]. This force is often employed to describe both atomic nuclei and neutron stars properties.

The pairing correlations are described with a zero range density dependent interaction of the following type:

$$V_{\mathrm{Pair}}(\mathrm{r}_i, \mathrm{r}_j) = V_0 \, g_{\mathrm{Pair}}[\rho_n(\mathrm{r}), \rho_p(\mathrm{r})] \, \delta(\mathrm{r}_{ij}) \,, \tag{3}$$

where $g_{\mathrm{Pair}}[\rho_n, \rho_p]$ is a functional of neutron and proton densities. In the calculations we use two different functionals for $g_{\mathrm{Pair}}[\rho_n(\mathrm{r}), \rho_p(\mathrm{r})]$. The first one, called below isoscalar (IS) pairing force, depends only on the total particle density, $\rho(r) = \rho_n(r) + \rho_p(r)$. Its expression is given by

$$g_{\mathrm{Pair}}[\rho_n(\mathrm{r}), \rho_p(\mathrm{r})] = 1 - \eta \left(\frac{\rho(r)}{\rho_0}\right)^\alpha \,, \tag{4}$$

where ρ_0 is the saturation density of the nuclear matter. This effective pairing interaction is extensively used in nuclear structure calculations and it was also employed for describing pairing correlations in the inner crust of neutron stars [5, 17–19]. The parameters are chosen to reproduce in infinite neutron matter two possible pairing scenarios [15], corresponding to a maximum gap of about 3 MeV (strong pairing scenario, hereafter named ISS) and, respectively, to a maximum gap around 1 MeV (weak pairing scenario, called below ISW). These two scenarios are simulated by two values of the pairing strength, i.e., V_0={-570,-430} MeV fm^{-3}. The other parameters are taken the same for the strong and the weak pairing, i.e., α=0.45, η=0.7 and ρ_0=0.16 fm^{-3}. The energy cut-off in the pairing tensor (8), necessary to cure the divergence associated to the zero range of the pairing force, was introduced through the factor $e^{-E_i/100}$ acting for $E_i > 20$ MeV, where E_i are the HFB quasiparticle energies.

The second pairing functional, referred below as isovector-isoscalar (IVS) pairing, depends explicitly on neutron and proton densities and has the following form [20]

$$g_{\mathrm{Pair}}[\rho_n(\mathrm{r}), \rho_p(\mathrm{r})] = 1 - \eta_s(1 - I(r)) \left(\frac{\rho(r)}{\rho_0}\right)^{\alpha_s} - \eta_n I(r) \left(\frac{\rho(r)}{\rho_0}\right)^{\alpha_n} \,, \tag{5}$$

where $I(r) = \rho_n(r) - \rho_p(r)$. As shown in Ref. [20], this pairing functional describes well the two-neutron separation energies and the odd-even mass differences in semi-magic nuclei. In the present calculations for this pairing functional we have used the parameters V_0= -703.86 MeV fm^{-3}, η_s=0.7115, α_s=0.3865, η_n=0.9727, α_n=0.3906, with the same cut-off prescription as for the IS pairing forces.

The pairing gaps in symmetric matter and neutron matter predicted by the three pairing forces introduced above are represented in Fig. 1 for a wide range of sub-nuclear densities. It can be seen that the IVS force gives a maximum gap closer to the strong isoscalar force.

For the zero range interactions introduced above and for spherically symmetric systems the radial HFB equations are given by

$$\begin{pmatrix} h(r) - \mu & \Delta(r) \\ \Delta(r) & -h(r) + \mu \end{pmatrix} \begin{pmatrix} U_i(r) \\ V_i(r) \end{pmatrix} = E_i \begin{pmatrix} U_i(r) \\ V_i(r) \end{pmatrix}, \tag{6}$$

where U_i, V_i are the upper and lower components of the radial HFB wave functions, μ is the chemical potential while $h(r)$ and $\Delta(r)$ are the mean field Hamiltonian and pairing field, respectively. They depend on particle density $\rho(r)$, abnormal pairing tensor $\kappa(r)$, kinetic energy density $\tau(r)$ and spin density $J(r)$ defined by:

$$\rho(r) = \frac{1}{4\pi} \sum_i (2j_i + 1) V_i^*(r) V_i(r) \tag{7}$$

$$\kappa(r) = \frac{1}{4\pi} \sum_i (2j_i + 1) U_i^*(r) V_i(r) \tag{8}$$

$$J(r) = \frac{1}{4\pi} \sum_i (2j_i + 1)[j_i(j_i + 1) - l_i(l_i + 1) - \frac{3}{4}] V_i^2 \tag{9}$$

$$\tau(r) = \frac{1}{4\pi} \sum_i (2j_i + 1)[(\frac{dV_i}{dr} - \frac{V_i}{r})^2 + \frac{l_i(l_i + 1)}{r^2} V_i^2] \tag{10}$$

The general expressions of the mean field in terms of the densities are given in Ref. [21]. The pairing field has a simple form, i.e.,

$$\Delta(r) = \frac{1}{2} g_{\text{Pair}}[\rho_n(r), \rho_p(r)] \, \kappa(r). \tag{11}$$

The HFB equations are solved in coordinate space and imposing the following boundary conditions at the border of the WS cells [6]: i) even parity wave functions vanish at $r = R_{WS}$;

ii) first derivatives of odd-parity wave functions vanish at $r = R_{WS}$. With these mixed boundary conditions at the cell border the continuous quasiparticle spectrum of the unbound neutrons is discretized.

Compared to the usual HFB calculations done for nuclei, in a WS cell the mean field of the protons has an additional contribution coming from the interaction of the protons with the electrons. Thus, the total proton mean field in the cell is given by

$$u^p(r) = u^{pp}_{\text{nucl}}(r) + u^{pp}_{\text{Coul}}(r) + u^{pe}_{\text{Coul}}(r), \tag{12}$$

where $u^{pp}_{\text{nucl}}(r)$ is the nuclear part of the mean field, given by the Skyrme interaction, while u^{pp}_{Coul} and u^{pe}_{Coul} are the mean fields corresponding to the Coulomb proton-proton and proton-electron interactions. The proton-proton Coulomb mean field has the standard form

$$u^{pp}_{\text{Coul}}(r) = e^2 \int d^3r' \, \rho_p(r') \frac{1}{|r - r'|} - e^2 \left(\frac{3}{\pi}\rho_p(r)\right)^{1/3}, \tag{13}$$

where the first and the second terms correspond, respectively, to the direct and the exchange part of proton-proton Coulomb interaction. The latter is evaluated in the Slater approximation.

The mean field corresponding to the proton-electron interaction is given by

$$u^{pe}_{\text{Coul}}(r) = -e^2 \int d^3r' \, \rho_e(r') \frac{1}{|r - r'|}. \tag{14}$$

Assuming that the electrons are uniformly distributed inside the cell, with the density $\rho_e = 3Z/(4\pi R^3_{WS})$, one gets

$$u^{pe}_{\text{Coul}}(r) = -2\pi e^2 \rho_e \left(R^2_{WS} - \frac{1}{3}r^2\right) = \frac{Ze^2}{2R_{WS}}\left(\left(\frac{r}{R_{WS}}\right)^2 - 3\right) \tag{15}$$

It can be seen that inside the WS cell the contribution of the proton-electron interaction to the mean field is quadratic in the radial coordinate.

B. The electron and the lattice energies

In the inner-crust the electrons are ultra-relativistic. Their kinetic energy is given by the expression [22]

$$T_e = Zm_ec^2\left\{\frac{3}{8x^3}\left[x\left(1 + 2x^2\right)\sqrt{1 + x^2} - \ln\left(x + \sqrt{1 + x^2}\right)\right] - 1\right\}, \tag{16}$$

where x is the relativistic parameter defined as $x = \hbar k_{Fe}/(m_e c^2)$. In the ultra-relativistic regime $x \gg 1$.

The lattice energy is generated by the electron-proton and electron-electron Coulomb interactions. The first one is given by

$$E_{Coul}^{pe} = - \int d^3 r d^3 r' \, \rho_p(r) \frac{e^2}{|r-r'|} \rho_e(r') = -\frac{3}{2} \frac{Z N_e e^2}{R_{WS}} + 2\pi \frac{e^2 N_e}{R_{WS}^3} \int dr \, \rho_p(r) r^4 \, , \qquad (17)$$

where the last two terms on the right hand side are obtained assuming that the electron density ρ_e is constant in the cell.

The electron-electron Coulomb energy is given by

$$E_{Coul}^{ee} = \frac{1}{2} \int d^3 r d^3 r' \, \rho_e(r) \frac{e^2}{|r-r'|} \rho_e(r') - \frac{3}{4} \left(\frac{3}{\pi} \right)^{1/3} e^2 \int d^3 r \, \rho_e^{4/3}(r) \qquad (18)$$

where the second term is the contribution of the exchange term evaluated in the Slater approximation. For a constant electron density one gets

$$E_{Coul}^{ee} = \frac{3}{5} \frac{N_e^2 e^2}{R_{WS}} \left(1 - \frac{5}{4} \left(\frac{3}{2\pi} \right)^{2/3} \frac{1}{N_e^{2/3}} \right) . \qquad (19)$$

The Coulomb energy corresponding to the proton-proton interaction is calculated within the mean field approach in a standard way, including the contribution of the exchange term evaluated in the Slater approximation.

III. BETA EQUILIBRIUM CONDITION

Beta equilibrium condition is satisfied if $\delta\mu = 0$ where

$$\delta\mu = m_e c^2 + \mu_e + m_p c^2 + \mu_p - m_n c^2 - \mu_n \, . \qquad (20)$$

The chemical potential of the electrons can be written as

$$\mu_e = \sqrt{(\hbar c k_e)^2 + (m_e c^2)^2} - m_e c^2 + \mu_I^{ee} + \mu_I^{ep}, \qquad (21)$$

where μ_I^{ee} and μ_I^{ep} are the contributions coming from the electron-electron and electron-proton interaction. They are given by:

$$\mu_I^{ee} = \frac{dE_{Coul}^{ee}}{dN_e} \qquad (22)$$

$$\mu_I^{ep} = \frac{dE_{Coul}^{ep}}{dN_e} \qquad (23)$$

The chemical potentials of the neutrons and protons are extracted from the HFB calculations. The contribution of the proton-electron interaction to the chemical potential of the protons is included through the proton-elecon mean field (14).

As seen in Eq. (12), the proton mean field includes also the contribution of the proton-electron interaction

The beta equilibrium condition can be satisfied exactly when the chemical potential of the neutrons, determined by the nonlocalized neutrons, is a continuous variable. In the calculations done here the neutron spectrum is discretized due to the boundary conditions imposed at the border of the cells (it is worth mentioning that this discretization has nothing to do with the discrete structure of the neutron spectrum generated by the symmetry of the crystal lattice). Consequently the beta equilibrium condition is satisfied only approximatively. In practice, we consider that the beta equilibrium condition is found when by changing the N/Z ratio the value of $\delta\mu$ is changing the sign. Then, from the two N/Z configurations for which $\delta\mu$ is changing the sign we keep the one which has the smaller binding energy. It is worth stressing that the beta equilibrium condition depends, through the discretization of the neutron spectrum, on the type of boundary conditions imposed at the border of the cells. How the type of boundary conditions could influence the structure of the cells is discussed in Ref [10].

IV.   RESULTS: THE STRUCTURE OF THE WIGNER-SEITZ CELLS

Within the framework presented in the previous sections we have determined the properties of the WS cells, i.e. the N/Z ratio and the radius of the cells. The calculations have been done for the set of baryonic densities shown in Table I. To find the structure of the cell at a given density we have considered all the configurations with the even number of protons between 12 and 60. For each number of protons we modified the radius of the cell with a step of 0.2 fm, keeping the same total density, until the number of neutrons included in the cell satisfies with the best accuracy the beta equilibrium condition. The most probable configuration at a given density is finally taken as the one with the lowest binding energy.

First we have determined the structure of the WS cells in the HF approximation, i.e., neglecting the contribution of pairing correlations. The results are given in Table II. Compared to previous calculations [6, 9] we find that the cells have a smaller number of protons.

Table II shows also that the number of protons are not anymore equal to a magic or a semi-magic number as in Ref.[6] (see Table I).

To understand better the results of Table II, in Fig. 2 we show the evolution of the binding energies per nucleon, calculated at beta equilibrium and at constant density, with respect to the proton number Z. The most probable configuration corresponds to the number of protons for which the binding energy has the lowest value. From Fig. 2 it can be seen that in the cells 1 and 2 there is a continuous decrease of the binding energy for the lowest values of Z. Thus, for these cells the HF calculations cannot predict a well-defined cell structure. From Fig. 2 it can be also seen that even for the cells in which one can identify a configuration with the lowest binding energy, the difference between this energy and the energy of other local minima is very small, of the order of 10 keV. The weak dependence of the binding energy on Z observed in Fig. 2 is caused by the almost exact compensation between the nuclear energy and the electron kinetic energy. This can be clearly seen in Fig. 3 where are shown, for the cells 2 and 6, the contributions to the total energy coming from the nuclear energy (dashed line) and the kinetic energy of the electrons (dashed-dotted line). It can be noticed that the local minima of nuclear binding energy at $Z = 20$ and $Z = 28$ are washed out by the kinetic energy of the electrons. The competition between the nuclear and Coulomb interaction, specific to the so-called frustrated systems, it is the reason why the structure of the WS cells it is not necessarily determined by the nuclear interaction and the associated nuclear shell effects.

A necessary condition for the validity of the WS approximation is the appearance in the neutron density of a well-defined plateau before the edge of the cell. From Fig. 4 (left pannel) it can be observed that this condition is hardly fulfilled for the cell 1, reasonably well for the cell 2 and better for the other cells.

We shall now discuss the effect of pairing correlations on the structure of the WS cells. To study the influence of pairing correlations we have performed HFB calculations with the three pairing interactions introduced in Section 3A. How the pairing correlations are distributed in the cells is illustrated in Fig.4 (right pannel) which shows the pairing fields of neutrons and protons for the force ISS. As expected, the pairing field profile has a non-uniform distribution which could be traced back to the density dependence of the pairing force [17]. The proton pairing field stays localized inside the nuclear cluster since a drip out of protons is not observed in our calculations. It can be noticed that for the cells 5 and 10,

with the proton numbers $Z = 20$ and $Z = 28$ (see Table III), the proton fields are zero. This indicates that in the nuclear clusters corresponding to these cells the proton numbers $Z = 20, 28$ behave as magic numbers, as in atomic nuclei.

The dependence of pairing energy on Z is illustrated in Fig. 3 (right pannel) for the cells number 2 and 6. One observes that in average the absolute value of the pairing energy is decreasing with Z, which shows that the dominant contribution to pairing comes from the nonlocalized neutrons (notice that for a cell the HFB calculations with various Z are done for a fixed total density).

The structure of the WS cells obtained in the HFB approach is given in Table III while in Fig. 5 it is shown the dependence of the binding energies, at beta equilibrium, on protons number. From Fig. 5 we observe that in the cell 1 the binding energy does not converge to a minimum before Z=12. For the cells 2-4 a minimum can be found for the ISW and/or IVS forces but this minimum is very close to the value of binding energy at Z=12. Therefore the structure of the cells 2-4 is ambiguous. The situation is different in the cells 5-10 where the binding energies converge to absolute minima located before Z=12. Thus for these cells the structure can be well-defined by the present HFB calculations.

Comparing Table III and Table II it can be observed that for the cells 6-9 the numbers of protons in the HF and HFB calculations differ by about 2 units. The largest difference, of 10 units, appears for the cell 5. However, as seen in Fig. 5, the HF minimum at Z=30 is in fact very close to the local minimum at Z=22. A similar situation can be noticed in cell 10 for the HF minima at Z=24 and Z=28. In conclusion, these calculations indicate that the pairing does not change much the structure of the low density cells 5-10. This could be also observed from the fact that in these cells the intensity of pairing force has only marginal effects on the proton and neutron numbers.

Let us now discuss more in detail what happens in the high density region for the configurations with small Z and small cells radii. When the radius of the cell becomes too small the boundary conditions imposed at the cell border through the WS approximation generate an artificial large distance between the energy levels of the nonlocalized neutrons. Consequently, the binding energy of the neutron gas is significantly underestimated. An estimation of how large could be the errors in the binding energy induced by the WS approximation

can be obtained from the quantity

$$f(\rho_n, R_{WS}) \equiv B_{inf.}(\rho_n) - B_{WS-inf.}(\rho_n, R_{WS}) , \qquad (24)$$

where the first term is the binding energy per neutron for infinite neutron matter of density ρ_n and the second term is the binding energy of neutron matter with the same density calculated inside the cell of radius R_{WS} and employing the same boundary conditions as in HF or HFB calculations. In Ref. [16] it was proposed for the finte size energy correction, Eq. 26, the following parametrisation

$$f(\rho_{n_g}, R_{WS}) = 89.05(\rho_{n_g}/\rho_0)^{0.1425} R_{WS}^{-2} , \qquad (25)$$

where ρ_{n_g} is the average density of neutrons in the gas region extracted from a calculation in which the cell contains both the nuclear cluster and the nonlocalized neutrons while ρ_0 is the nuclear matter saturation density.

How the energy corrections described by Eq.(25) influences the HF (HFB) results can be seen in Tables III (Tables-IV) and Fig. 2 (Fig. 5). As expected, the influence of the corrections is more important for the cells 1-5, in which the neutron gas has a higher density, and for those configurations corresponding to small cell radii. For the cell 1 the binding energy after the correction is still decreasing for the smallest Z values, which means that the structure of this cell remains uncertain. The structure of the cells 2-4 can be now determined for all pairing forces. However, as seen in Fig. 5, for these cells the absolute minima are still very close to the binding energies at Z=12 which shows that the structure of these cells remains ambiguous even after the energy correction.

V.   SUMMARY AND CONCLUSIONS

In this paper we have examined the influence of pairing correlations on the structure of inner crust of neutron stars. The study was done for the region of the inner crust which is supposed to be formed by a lattice of spherical clusters. The lattice was treated as a set of independent cells described in the Wigner-Seitz approximation. To determine the structure of a cell we have used the nuclear binding energy given by the HFB approach. For the HFB calculations we have considered a particle-hole interaction of Skyrme type (SLy4) while as particle-particle interaction we have used three zero range density-dependent pairing

12

forces of various intensities. The calculations show that the pairing correlations have a weak influence on the structure of WS cells.

For the cells with high density and small radii the binding energies do not converge to a minimum when the proton number has small values. We believe that the reason for that is the failure of the WS approximation when the cell radius is too small. For a small radius of the cell the average distance between the energy levels of the nonlocalised neutrons becomes artificially large which cause an underestimation of the binding energy. To correct this drawback we have used an empirical expression based on the comparison between the binding energy of neutrons calculated in infinite matter geometry and in a spherical cell [16]. We found that the corrections to the binding energies are significant for the high density cells with small proton numbers. This show that the WS approximation is not accurately enough for predicting the structure of the high density region of the inner crust.

Acknowledgements

[1] N. K. Glendenning, *Compact Stars* (Springer 1997)

[2] P. Haensel, A. Y. Potekhin, D. G. Yakovlev, *Neutron Stars I* (Springer 2007)

[3] D. Page, U. Geppert & F. Weber, Nucl. Phys. **A 777**, p. 497-530 (2006); D. Page & S. Reddy, Annu. Rev. Nucl. & Part. Sci. **56**, 327 (2006)

[4] P.M. Pizzochero, F. Barranco, E. Vigezzi, and R. A. Broglia, Astrophys. J. **569**, 381 (2002)

[5] C. Monrozeau, J. Margueron, and N. Sandulescu, Phys. Rev. C **75**, 065807 (2007)

[6] J. W. Negele and D. Vautherin, Nucl. Phys. **A207**, 298 (1973).

[7] J. W. Negele and D. Vautherin, Phys. Rev. **C 5**, 1472 (1972)

[8] J. W. Negele, Phys. Rev. **C 1**, 1260 (1970); X. Campi and D. W. L. Sprung, Nucl. Phys. **A 194**, 401 (1972)

[9] M. Baldo, U. Lombardo, E. E. Saperstein, S. V. Tolokonnikov, Nucl. Phys. A 750, 409 (2005); M. Baldo et al, Eur.Phys.J.A32:97-108,2007

[10] M. Baldo, E. E. Saperstein, S. V. Tolokonnikov, Nucl. Phys. A 775, 235 (2006)

[11] S. A. Fayans, S. V. Tolokonnikov, E. L. Trykov, and D. Zaisha, Nucl. Phys. A 676, 49 (2000)

[12] K. Oyamatsu, Nuclear Physics A561 (1993) 431

[13] N. Chamel, S. Goriely, J. M. Pearson, and M. Onsi, Phys. Rev. **C 81**, 045804 (2010)

[14] E. Chabanat, P. Bonche, P. Haensel, J. Meyer, and R. Schaeffer, Nucl. Phys. A623, 710 (1997)

[15] U. Lombardo, in *Nuclear Methods and the Nuclear Equation of State*, edited by M. Baldo (World Scientific, Singapore, 1999), pp. 458-510.

[16] J. Margueron, N. Van Giai, N. Sandulescu, Proceeding of the International Symposium EX-OCT07, "Exotic States of Nuclear Matter", Edited by U. Lombardo et al., World Scientific (2007); arXiv:0711.0106

[17] N. Sandulescu, N. Van Giai, and R. J. Liotta, Phys. Rev. C **69**, 045802 (2004).

[18] N. Sandulescu, Phys. Rev. C **70**, 025801 (2004) .

[19] N. Sandulescu, Eur. Phys. J. (Special Topics) **156**, 265 (2008).

[20] J. Margueron, H. Sagawa, and K. Hagino, Phys. Rev. C76, 064316 (2007); J. Margueron, H. Sagawa, and K. Hagino, Phys. Rev. C77, 054309 (2008)

[21] J. Dobaczewski, H. Flocard, Treiner, Nucl. Phys A422, 103 (1984)

[22] L. Landau, *Statistical Physics* (Springer-Verlag 1983)

N_{cell}	ρ	N	Z	R_{WS}
	[g cm^{-3}]			[fm]
1	7.9 10^{13}	1460	40	20
2	3.4 10^{13}	1750	50	28
3	1.5 10^{13}	1300	50	33
4	9.6 10^{12}	1050	50	36
5	6.2 10^{12}	900	50	39
6	2.6 10^{12}	460	40	42
7	1.5 10^{12}	280	40	44
8	1.0 10^{12}	210	40	46
9	6.6 10^{11}	160	40	49
10	4.6 10^{11}	140	40	54

TABLE I: The structure of the Wigner-Seitz cells determined in Ref.[6]. ρ is the baryon density, N and Z are the numbers of neutrons and protons while R_{WS} is the radius of the cell. Compared to Ref. [6] here it is not shown the cell with the highest density located at the interface with the pasta phase.

N_{cell}	ρ [g cm^{-3}]	N	Z	R_{WS} [fm]	E/A [MeV]	E_N/A [MeV]	T_e/A [MeV]	μ_n [MeV]	μ_p [MeV]
3	$1.5\ 10^{13}$	318	16	20.8	3.021	1.409	1.622	4.591	−38.03
4	$9.6\ 10^{12}$	322	18	24.2	2.313	0.724	1.600	4.169	−35.94
5	$6.2\ 10^{12}$	528	30	33.0	1.716	0.310	1.409	2.996	−31.22
6	$2.6\ 10^{12}$	252	22	34.6	0.735	−1.047	1.805	1.886	−27.49
7	$1.5\ 10^{12}$	158	22	36.6	0.139	−2.413	2.590	1.025	−26.90
8	$1.0\ 10^{12}$	120	24	38.6	−0.252	−3.649	3.447	0.773	−26.27
9	$6.6\ 10^{11}$	80	24	39.8	−0.722	−5.294	4.643	0.294	−26.07
10	$4.6\ 10^{11}$	58	24	41.4	−1.260	−6.812	5.648	−0.312	−26.06

TABLE II: The structure of Wigner-Seitz cells obtained in the HF approximation with the force SLy4. E/A, E$_N$/A and T$_e$/A are, respectively, the total energy, the nuclear energy and the electron kinetic energy per baryon while μ_n and μ_p are the neutron chemical potential and the proton chemical potential. The other quantities are the same as in Table I. The structure of the cells 1-2 it is not shown because it is not well-defined by the present HF calculations.

N_{cell}	N			Z			R_{WS} [fm]			E/A [MeV]			μ_n [MeV]			μ_p [MeV]
	ISW	ISS	IVS	ISW	ISS	IVS	ISW	ISS	IVS	ISW	ISS	IVS	ISW	ISS	IVS	ISW
2	476			18			18.0			4.607			6.915			−46.95
3	368		378	16		16	21.8		20.0	2.995		2.734	4.864		4.395	−37.76
4	330		460	18		22	24.4		27.2	2.302		2.059	3.820		3.431	−35.71
5	320	336	344	20	20	20	28.0	28.4	28.6	1.685	1.604	1.473	2.974	2.828	2.629	−32.57
6	300	242	238	24	22	22	36.6	34.2	34.0	0.725	0.691	0.636	1.631	1.678	1.546	−32.45
7	202	170	174	26	24	24	39.6	37.6	37.8	0.131	0.121	0.078	1.152	1.052	0.988	−25.98
8	120	118	120	24	24	24	38.6	38.4	38.6	−0.262	−0.268	−0.300	0.607	0.696	0.654	−28.56
9	92	90	94	26	26	26	41.4	41.4	41.6	−0.739	−0.748	−0.776	0.402	0.384	0.403	−25.51
10	84	72	64	28	28	26	46.0	44.2	42.6	−1.282	−1.283	−1.310	0.238	0.167	0.092	−23.29

TABLE III: The structure of Wigner-Seitz cells obtained in the HFB approximation. The results corresponds to the isoscalar weak (ISW), isoscalar strong (ISS) and isovector-isoscalar (IVS) pairing forces. The displayed quantities are the same as in Table II. In the table are shown only the structures of the cells which could be well-defined by the HFB calculations.

N_{cell}	N	Z	R_{WS} [fm]	E/A [MeV]	E_N/A [MeV]	T_e/A [MeV]	μ_n [MeV]	μ_p [MeV]
2	474	20	18.0	4.850	2.935	1.713	6.046	−47.49
3	980	40	30.2	3.121	1.806	1.241	4.651	−37.01
4	726	30	31.6	2.387	1.246	1.088	3.953	−31.67
5	538	30	33.2	1.762	0.344	1.376	3.080	−31.17
6	252	22	34.6	0.771	−1.047	1.805	1.886	−27.49
7	158	22	36.6	0.167	−2.413	2.590	1.025	−26.90
8	120	24	38.6	−0.228	−3.649	3.447	0.773	−26.27
9	80	24	39.8	−0.702	−5.294	4.643	0.294	−26.07
10	58	24	41.4	−1.257	−6.812	5.648	−0.312	−26.06

TABLE IV: The structure of the Wigner-Seitz cells obtained in the HF approximation including the finite size corrections (see text for details). The displayed quantities are the same as in Table II.

N_{cell}	N			Z			R_{WS} [fm]			E/A [MeV]			μ_n [MeV]			μ_p [MeV]
	ISW	ISS	IVS	ISW	ISS	IVS	ISW	ISS	IVS	ISW	ISS	IVS	ISW	ISS	IVS	ISW
2	656	676	656	22	22	22	20.0	20.2	20.0	4.804	4.582	4.603	6.958	6.785	6.785	−45.60
3	718	454	734	28	20	28	27.2	23.4	27.4	3.095	2.932	2.833	4.933	4.492	4.472	−35.93
4	712	460	594	30	22	28	31.4	27.2	29.6	2.370	2.256	2.122	3.714	3.607	3.446	−37.67
5	320	336	344	20	20	20	28.0	28.4	28.6	1.749	1.666	1.534	2.974	2.828	2.629	−32.57
6	300	242	238	24	22	22	36.6	34.2	34.0	0.758	0.729	0.674	1.631	1.678	1.546	−32.45
7	202	170	174	26	24	24	39.6	37.6	37.8	0.156	0.148	0.106	1.152	1.052	0.988	−25.98
8	120	118	120	24	24	24	38.6	38.4	38.6	-0.238	-0.244	-0.276	0.607	0.696	0.654	−28.56
9	92	90	94	26	26	26	41.4	41.2	41.6	-0.721	-0.730	-0.758	0.402	0.384	0.403	−25.51
10	84	72	64	28	28	26	46.0	44.2	42.6	-1.268	-1.283	-1.310	0.238	0.167	0.092	−23.29

TABLE V: The structure of Wigner-Seitz cells obtained in the HFB approximation including the finite size corrections. The displayed quantities are the same as in Table III.
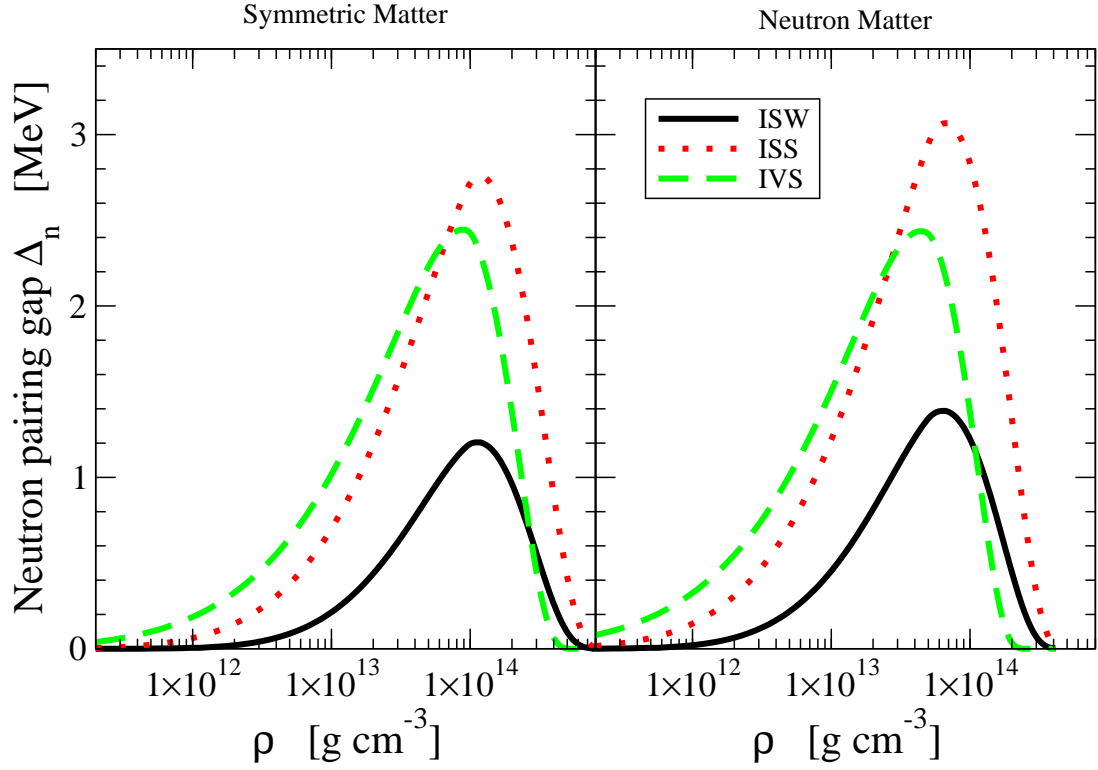
FIG. 1: (color online) Neutron pairing gap for the interactions ISW (isoscalar weak), ISS (isoscalar strong) and IVS (isovector-isoscalar) in symmetric nuclear matter and in neutron matter.
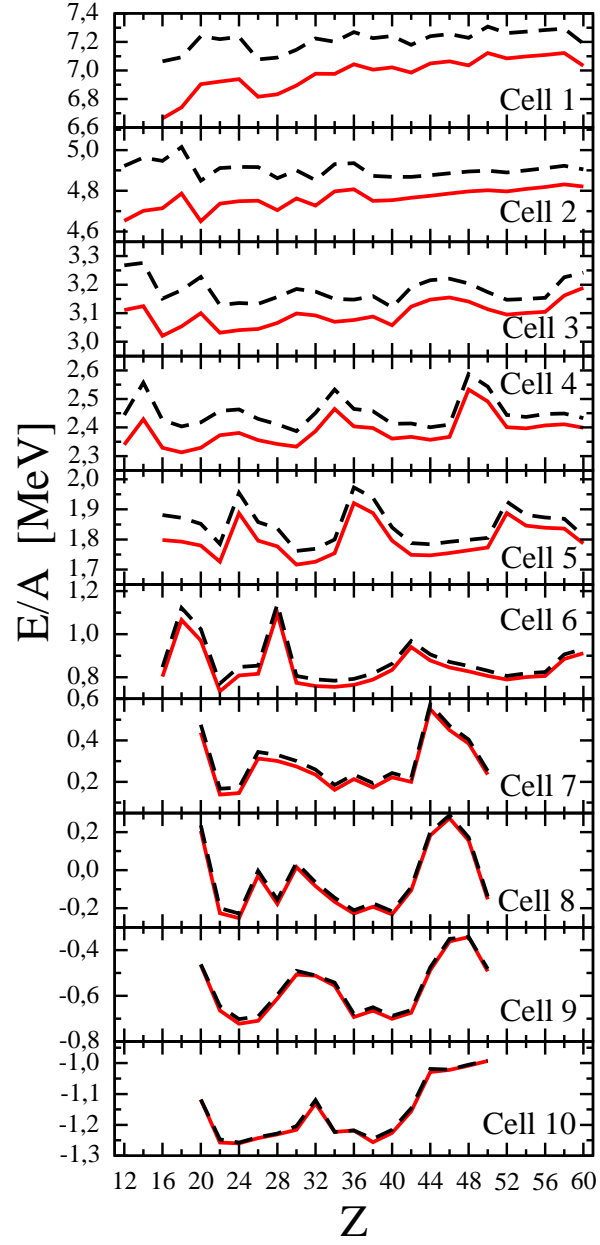
FIG. 2: (color online) HF energies per particle versus the proton number Z (full lines). With the dashed lines are represented the HF results after the finite size corrections.
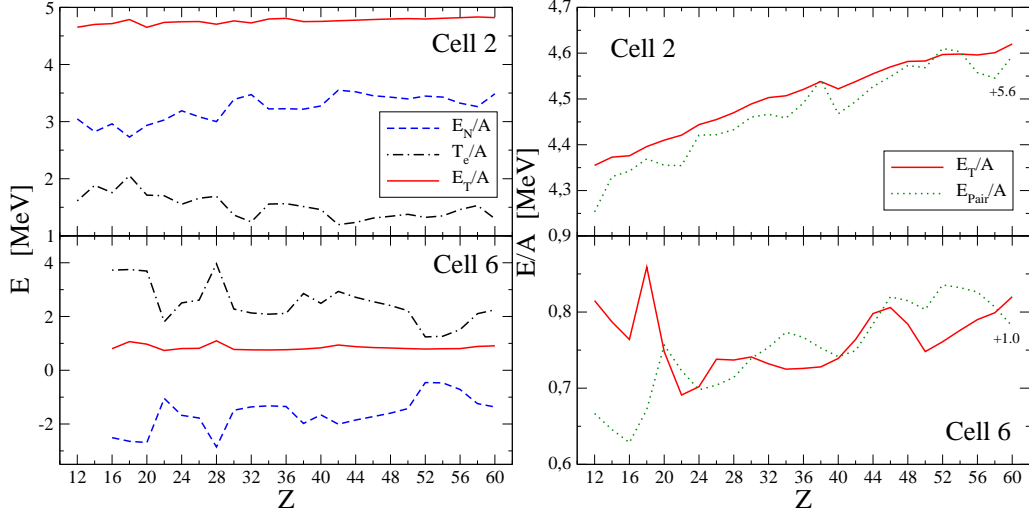
FIG. 3: (color online) The different contributions to the total energy in the cells 2 and 6 for the HF (left pannel) and HFB (right pannel) calculations. Are shown: the total energy (solid line), the nuclear energy (dashed line), the kinetic energy of the electrons (dashed-dotted line), and the pairing energy for the ISS pairing interaction (dotted line). The pairing energies are shifted up as indicated in the figure.
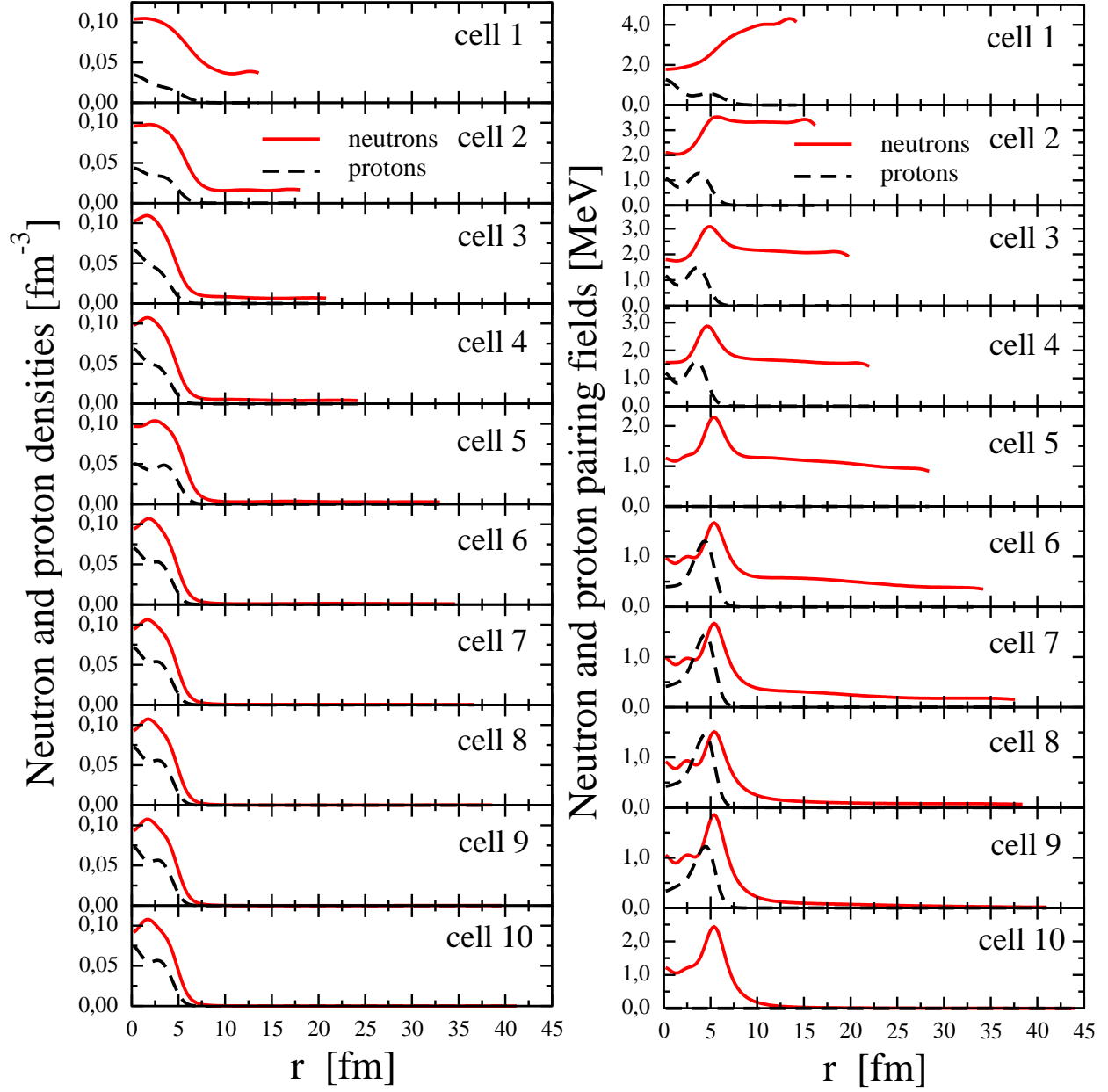
FIG. 4: (color online) The radial profiles of densities (left) and pairing fields (right) for neutrons (full lines) and protons (dashed lines) . The densities correspond to the HF calculations while the pairing fields to the HFB calculations with the pairing force ISS.
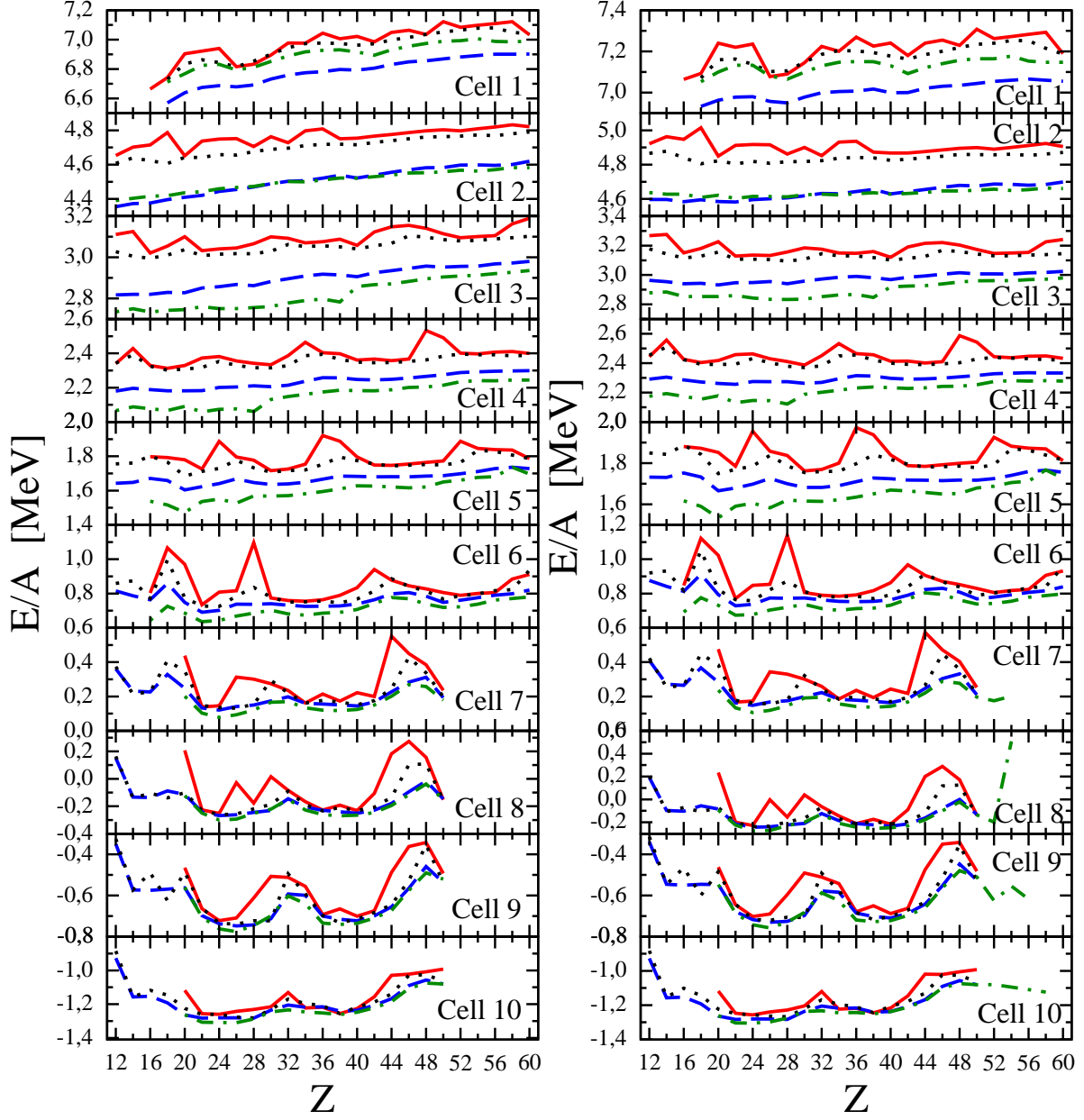
FIG. 5: (color online) The HFB energies per particle as function of proton number for the pairing forces ISW (dotted line), ISS (dashed line) and IVS (dashed-dotted line). The solid lines represent the HF results. In the left pannel are shown the results obtained including the finite size corrections.